ADVANCES IN ATMOSPHERIC SCIENCES, VOL. 36, JUNE 2019, 603–613

• **Original Paper** •

Evaluation of Simulated CO_2 Concentrations from the CarbonTracker-Asia Model Using In-situ Observations over East Asia for 2009–2013

Samuel Takele KENEA*[1], Young-Suk OH[1], Jae-Sang RHEE[1], Tae-Young GOO[1], Young-Hwa BYUN[1], Shanlan LI[1], Lev D. LABZOVSKII[1], Haeyoung LEE[2], and Robert F. BANKS[3]

[1]*Climate Research Division, National Institute of Meteorological Sciences,* 33, *Seohobuk-ro, Seogwipo-si, Jeju-do,* 63568*, Republic of Korea*

[2]*Environmental Meteorology Research Division, National Institute of Meteorological Sciences,* 33, *Seohobuk-ro, Seogwipo-si, Jeju-do,* 63568*, Republic of Korea*

[3]*Meteorology Department, Delta Air Lines, Inc., Atlanta GA, United States*

(Received 24 July 2018; revised 10 December 2018; accepted 25 February 2019)

ABSTRACT

The CarbonTracker (CT) model has been used in previous studies for understanding and predicting the sources, sinks, and dynamics that govern the distribution of atmospheric CO_2 at varying ranges of spatial and temporal scales. However, there are still challenges for reproducing accurate model-simulated CO_2 concentrations close to the surface, typically associated with high spatial heterogeneity and land cover. In the present study, we evaluated the performance of nested-grid CT model simulations of CO_2 based on the CT2016 version through comparison with in-situ observations over East Asia covering the period 2009–13. We selected sites located in coastal, remote, inland, and mountain areas. The results are presented at diurnal and seasonal time periods. At target stations, model agreement with in-situ observations was varied in capturing the diurnal cycle. Overall, biases were less than 6.3 ppm on an all-hourly mean basis, and this was further reduced to a maximum of 4.6 ppm when considering only the daytime. For instance, at Anmyeondo, a small bias was obtained in winter, on the order of 0.2 ppm. The model revealed a diurnal amplitude of CO_2 that was nearly flat in winter at Gosan and Anmyeondo stations, while slightly overestimated in the summertime. The model's performance in reproducing the diurnal cycle remains a challenge and requires improvement. The model showed better agreement with the observations in capturing the seasonal variations of CO_2 during daytime at most sites, with a correlation coefficient ranging from 0.70 to 0.99. Also, model biases were within −0.3 and 1.3 ppm, except for inland stations (7.7 ppm).

Key words: model evaluation, in-situ observations, CarbonTracker, East Asia

Citation: Kenea, S. T., and Coauthors, 2019: Evaluation of simulated CO_2 concentrations from the CarbonTracker-Asia model using in-situ observations over East Asia for 2009–2013. *Adv. Atmos. Sci.*, **36**(6), 603–613, https://doi.org/10.1007/s00376-019-8150-x.

Article Highlights:

- Model-simulated CO_2 concentrations are evaluated with in-situ observations at diurnal and seasonal time scales.
- The model performs better in reproducing the daytime CO_2 concentrations than the nighttime.
- The model captures well the seasonal variations of CO_2 concentrations during daytime at most sites.

1. Introduction

Atmospheric carbon dioxide (CO_2) is a key greenhouse gas that causes global warming (IPCC, 2013). The increase of the CO_2 concentration, on average 2 ppm yr^{-1} globally, is significantly related with contribution from human activities. In fact, the relative contribution of CO_2 to the atmosphere varies greatly with region. East Asia is an important region that emits a large amount of CO_2 into the atmosphere (Tian et al., 2016). On the other hand, the sink of CO_2 is predominantly controlled by terrestrial vegetation uptake via photosynthesis and oceanic uptake (Keeling et al., 1989; Hansen et al., 2007; Watson et al., 2011).

Accurate estimates of CO_2 sources and sinks are of great importance for validating carbon emissions reduction efforts and reducing the uncertainties of carbon cycle–climate feedbacks. Efforts have been undertaken to reduce the uncertainty of model estimations of fluxes through the assimilation of accurate observations of CO_2 data from the global network (Tans et al., 1990; Gurney et al., 2002). However, as previous studies point out, there are uncertainties in terms of the localization of sources and sinks on regional scales (e.g. Baker et al., 2006). Owing to less spatial coverage of accu-

* Corresponding author: Samuel Takele KENEA
Email: samueltake@yahoo.ca

rate observations of CO_2 over East Asia, the regional CO_2 fluxes estimated from atmospheric inversions are still uncertain (e.g., Swathi et al., 2013). In addition, uncertainties in the planetary boundary layer height, or in horizontal winds, affect the modeled near-surface CO_2 concentrations (Gurney et al., 2002; Lin and Gerbig, 2005; Gerbig et al., 2008; Prather et al., 2008; Ahmadov et al., 2009). Therefore, continuous assessment and evaluation of model simulations of CO_2 concentrations against accurate in-situ observations is vital.

Recently, the nested-grid CarbonTracker (CT)-Asia model was run using versions CT2013B (Cheng et al., 2013) and CT2016 (documented at http://carbontracker.noaa.gov, Peters et al., 2007) by the National Institute of Meteorological Sciences (NIMS), Republic of Korea. In this simulation, in-situ continuous hourly CO_2 concentrations (including daytime and nighttime) at Ryori, Minamitorishima, Yonagunijima, and Tae-ahn Peninsula, which are close to Anmyeondo station, and CONTRAIL (Comprehensive Observation Network for Trace gases by Airliner) data were assimilated. This result could be used as an indicator for where the model needs improvement in order to estimate accurate fluxes through accurate estimates of flux error in the assimilation process.

In the present study, we investigated the spatiotemporal distribution of simulated near-surface CO_2 concentrations along with CO_2 fluxes from fossil fuel emissions and the biosphere. Then, we statistically evaluated the model's performance in reproducing diurnal and seasonal variations of near-surface CO_2 concentrations through comparison with in-situ observations over target stations. We also examined the wind speed and directions over the target stations during daytime and nighttime for both the winter and summer seasons.

2. Sites

The stations used to evaluate the model's performance in simulating near-surface CO_2 concentrations were as follows (sufficient information on the stations is provided in the literature, some examples of which are cited): the coastal stations of Anmyeondo, Gosan, and Ryori (Sasaki, 2006); the remote stations of Yonagunijima (Fukuyama, 2013) and Minamitorishima; the mountain sites of Mt. Waliguan (Zhou et al., 2004, 2006) and Lulin (Qu et al., 2013); and the inland stations of Kisai and Shangdianzi (Cheng et al., 2018). These sites are located under different vegetation types, climate features, and economic zones (e.g., Fang et al., 2014; Cheng et al., 2018). Figure 1 displays a map of the stations overlaid on a spatial plot of the terrain height.

3. Data and methods

3.1. *CT inverse model*

CT is an inverse atmospheric model developed by the National Oceanic and Atmospheric Administration Earth System Research Laboratory Global Monitoring Division (http://www.esrl.noaa.gov/gmd/ccgg/carbontracker). Here, we adopt a nested-grid CT inverse model with a horizontal resolution of $1^\circ \times 1^\circ$ for the simulation of atmospheric CO_2 concentrations over East Asia. Model simulations were run by NIMS based on the CT2016 version. The model uses Transport Model 5 (Krol et al., 2005), forced by meteorological fields from ERA-Interim (Dee et al., 2011). The model gives four components of CO_2 signals, which respectively derive from fossil fuel emissions, air–sea CO_2 exchange, and terrestrial fluxes from wildfire emissions and non-fire net ecosystem exchange. The model uses the a priori information for surface CO_2 flux data for each module. The biosphere CO_2 flux is supplied by a biosphere model, CASA (the Carnegie–Ames Stanford Approach). In the fire module, CO_2 released by fire is taken from the Global Fire Emission Database, version 4.1s, at a three-hourly temporal resolution. We used two different fossil fuel CO_2 emissions datasets—namely, "Miller" and ODIAC (Open Source Data Inventory for Anthropogenic CO_2)—which were used to help assess the uncertainty in the mapping process. In the ocean module, prior estimates of air–sea CO_2 flux were determined from the Ocean Inversion Fluxes scheme, and the updated version of the Takahashi et al. (2009) pCO2 climatology. Further details are provided in the CT document (CT2016 release, https:/www.esrl.noaa.gov/gmd/ccgg/carbontracker/CT2016_doc.php). While obtaining CO_2 signals from oceanic and terrestrial biospheric surface fluxes, we used data from Tae-ahn Peninsula, Minamitorishima, Yonagunjima, and Ryori for optimizing those fluxes in the assimilation process. The model uses an ensemble Kalman filter to estimate the surface CO_2 flux with atmospheric CO_2 measurements as a constraint (Peters et al., 2007, 2010).

3.2. *In-situ measurements*

In-situ measurements of CO_2 concentrations were taken using non-dispersive infrared (NDIR) absorption sensors and cavity ring-down analyzers (CRDS). Measurements derived from both instruments were used for evaluating the model's ability to simulate diurnal and seasonal variations of near-surface CO_2 concentrations. The accuracy of CO_2 measurements from those systems is typically better than 0.1 ppm (Andrews et al., 2014). All sites used in this study only have one air intake height. More information concerning the sites can be found at http://www.esrl.noaa.gov/gmd/ccgg/insitu/. The in-situ data were obtained from the World Data Centre for Greenhouse Gases (WDCGG) (https://ds.data.jma.go.jp/gmd/wdcgg/cgi-bin/wdcgg/catalogue.cgi), which operates under the framework of the WMO's Global Atmosphere Watch. Simultaneous measurements of meteorological parameters, such as atmospheric temperature, wind speed and direction, and relative humidity, were also provided by the WDCGG. In this work, surface sampling stations were chosen at inland, coastal, mountainous, and remote sites (see Fig. 1 and Tables 1 and 2 for more information).

3.3. *Comparison method*

To evaluate the performance of the model's ability in simulating CO_2 concentrations through comparison with in-situ observations, we first applied temporal and spatial coinci-

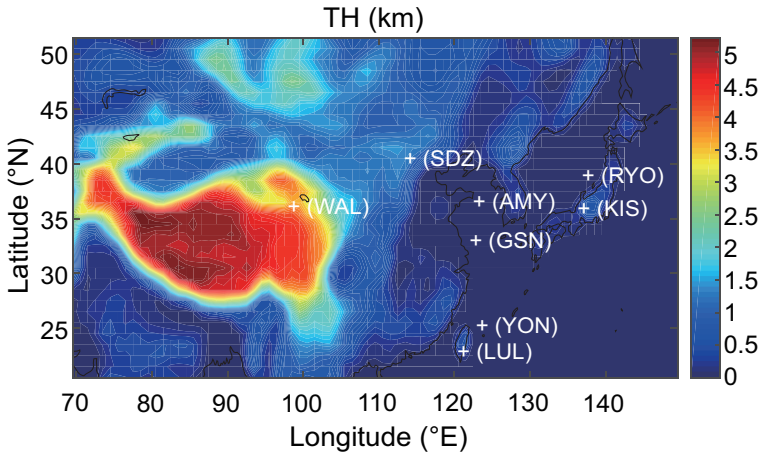

Fig. 1. Terrain height (units: km) with an overlay map of the network of in-situ measurement stations, where the three-letter abbreviations mean the following: WAL, Mt. Waliguan; SDZ, Shangdianzi; AMY, Anmyeondo; RYO, Ryori; KIS, Kisai; GSN, Gosan; YON, Yonagunijima; LUL, Lulin. The data are obtained from CT model.

Table 1. Details of the instruments at selected stations.

Station name	Lab	Method	Sampling type	Latitude/longitude	Height AMSL	Sampling height
Anmyeondo	KMA	NDIR (2009–11), CRDS (2012–13)	Continuous	36.538/126.33	46.0	40.0
Gosan	NIER	NDIR	Continuous	37.17/126.10	72.0	10.0
Minamitorishima	JMA	NDIR	Continuous	24.28/153.98	8.0	20.0
Ryori	JMA	NDIR	Continuous	39.03/141.82	260.0	20.0
Yonagunjima	JMA	NDIR	Continuous	24.47/123.02	30.0	20.0
Kisai	Saitama	NDIR	Continuous	36.08/139.55	13.0	20.0
Lulin	NOAA/ESRL	NDIR	Flask	23.47/120.87	2867.0	—
Mt. Waliguan	CMA	CRDS	Continuous	36.28/100.90	3810.0	80.0
Shangdianzi	CMA NOAA/ESRL	NDIR	Flask	40.65/117.12	287.0	—

Notes: KMA, Korea Meteorological Agency; NIER, National Institute of Environmental Research; JMA, Japan Meteorological Agency; CMA, China Meteorological Administration; NOAA/ESRL, National Oceanic and Atmospheric Administration's Earth System Research Laboratory; NDIR, non-dispersive infrared sensors; CRDS, cavity ring-down analyzers; AMSL, above mean sea level.

dence criteria over all selected stations. Model outputs were sampled at the nearest grid point and the model vertical level that corresponded to the in-situ inlet height of the stations. In fact, there were other methods/techniques that we could have applied for the spatial coincidence criteria, such as the nearest grid point method, interpolation with concentration slope or linear interpolation, and grid-averaging, but they were found to affect the correlations between the simulated and observed results, particularly at coastal and inland stations. This finding is consistent with Patra et al. (2008). In evaluating the model's performance at seasonal time scales, we considered daytime (1330–1630 LST), nighttime, and all-hourly averaged data. In addition, we investigated the amplitude and phase of the seasonal cycle, and quantitatively determined the Pearson's correlation coefficient (R) between simulations and observations. Linear regression analysis was applied to examine how the data were spread over the linear fitting. We also assessed the model's ability to reproduce the diurnal variations of the observations by comparing the phase and amplitude of the diurnal cycle. The bias was expressed as the difference between simulation and observation.

4. Results and discussion

We compared the downscaled CT model-simulated atmospheric CO_2 concentration based on CT2016 versions with in-situ observations over East Asia. Here, we discuss the comparison of CO_2 at diurnal and seasonal time scales.

4.1. *Spatiotemporal distribution of CO_2 concentrations*

Here, we highlight the spatiotemporal variations of the simulated near-surface CO_2 concentrations and fluxes during the period 2009–13. The distribution of the multi-year seasonal mean near-surface CO_2 concentrations in East Asia shows significant spatial heterogeneity. The spatial and temporal variations of near-surface CO_2 concentrations were pre-

dominantly driven by the anthropogenic emissions, and by the variations of the biospheric CO_2, resulting from the seasonal phenomena of growth and decay of land vegetation, as well as atmospheric transport. The surface-level simulated CO_2 concentration was maximum in winter and minimum in summer. Figure 2 displays the simulated near-surface atmospheric CO_2 concentrations for each season over East Asia in the period 2009–13, while Fig. 3 shows the CO_2 fluxes derived from fossil fuels and biogenic emissions in different seasons. The seasonal spatial distribution of the simulated CO_2 concentrations had a consistent pattern with that of the spatial distribution of CO_2 fluxes from fossil fuel emissions and the biosphere over East Asia (20°–51°N, 90°–150°E). The hot spots of higher fossil-fuel fluxes (see Fig. 3, top panel) were located over a region encompassing the megacities of Korea, Japan, and eastern China, which is a recognized region of high CO_2 emissions (e.g., Ballav et al., 2012; Shim et al., 2013).

4.2. *Diurnal cycle of CO_2*

Validating the amplitude of the diurnal variability of the model simulation through comparison with in-situ near-surface observations is vital, as the diurnal variability of near-surface CO_2 represents the sources, sinks, and related surface processes (e.g., Bakwin et al., 1998). The phenomena of photosynthesis and respiration, boundary layer dynamics, and pollution transport are key factors for the observed diurnal cycles of CO_2 concentrations near the surface (Bakwin et al., 1998). Law et al. (2008) examined model simulations of CO_2 concentrations along with observational data and found that the diurnal amplitude errors were contributed by sampling choice in the vertical and horizontal directions, the model resolutions, and the land surface flux.

Figures 4 and 5 provide a comparison of the in-situ and model-simulated diurnal variations of atmospheric CO_2 concentrations during winter and summer over the course of the study period for the following four stations: Anmyeondo, Gosan, Ryori, and Kisai. The overall patterns of the diurnal cycles of the simulated CO_2 concentrations followed the observations during daytime, but with large discrepancy during nighttime. Pronounced diurnal cycles of CO_2 were present in summertime, with peaks at night and troughs in the afternoon. The bias, as shown in Table 2, was less than 6.3 ppm on the all-hourly mean basis, and this bias was further reduced to a maximum of 4.6 ppm (see Table 3) when considering only daytime.

Looking specifically at Anmyeondo and Gosan stations, the model result agreed well with observations in that both showed no distinct diurnal cycle. At Anmyeondo, there was an estimated small positive bias of the model simulation (0.2 ppm) against the in-situ observations during winter. In summertime, the bias was 3.6 ppm. Representation error is subject to flux gradients and the direction of land or sea breezes (Tolk et al., 2008). Although the flux gradient was high over Anmyeondo in winter (see Fig. 3), a small bias was estimated. As evident in the wind rose plot in Fig. S1 in the Electronic Supplementary Material (ESM), there was a strong influence of sea breezes bringing ocean airmasses containing depleted CO_2. We can infer that, to a large extent, such a phenomenon was captured well by the model.

On the other hand, the relative influence of local and regional emissions might have been strong in summer, since

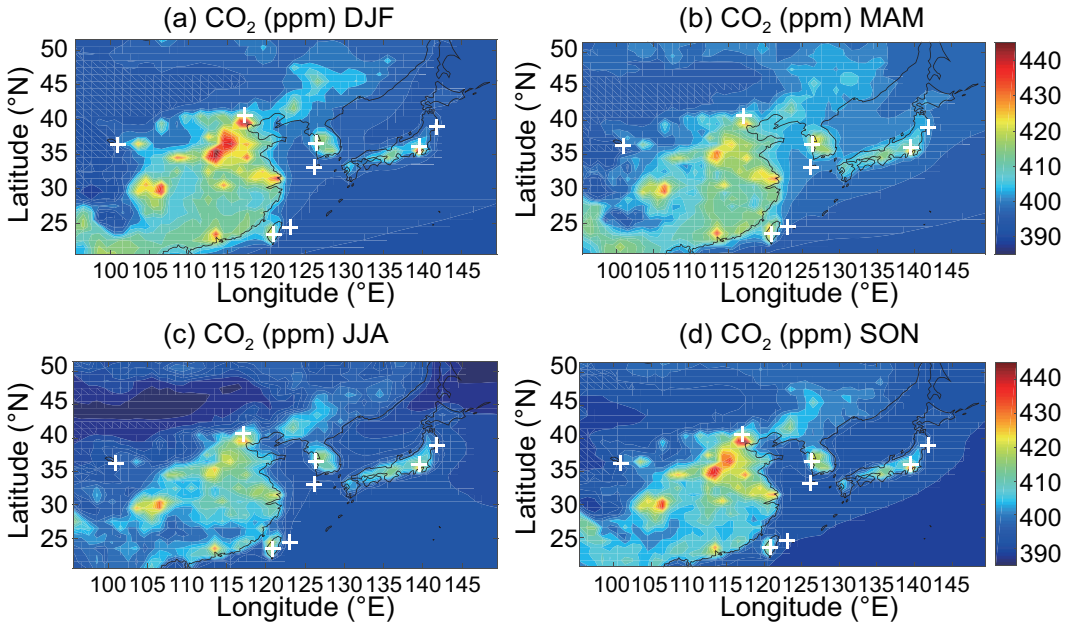

Fig. 2. Model-simulated seasonal mean near-surface CO_2 concentrations (units: ppm) during 2009–13. Plus signs denote the in-situ observation stations used in the study; DJF, MAM, JJA and SON denote the winter (December–February), spring (March–May), summer (June–August) and autumn (September–November) seasons, respectively.

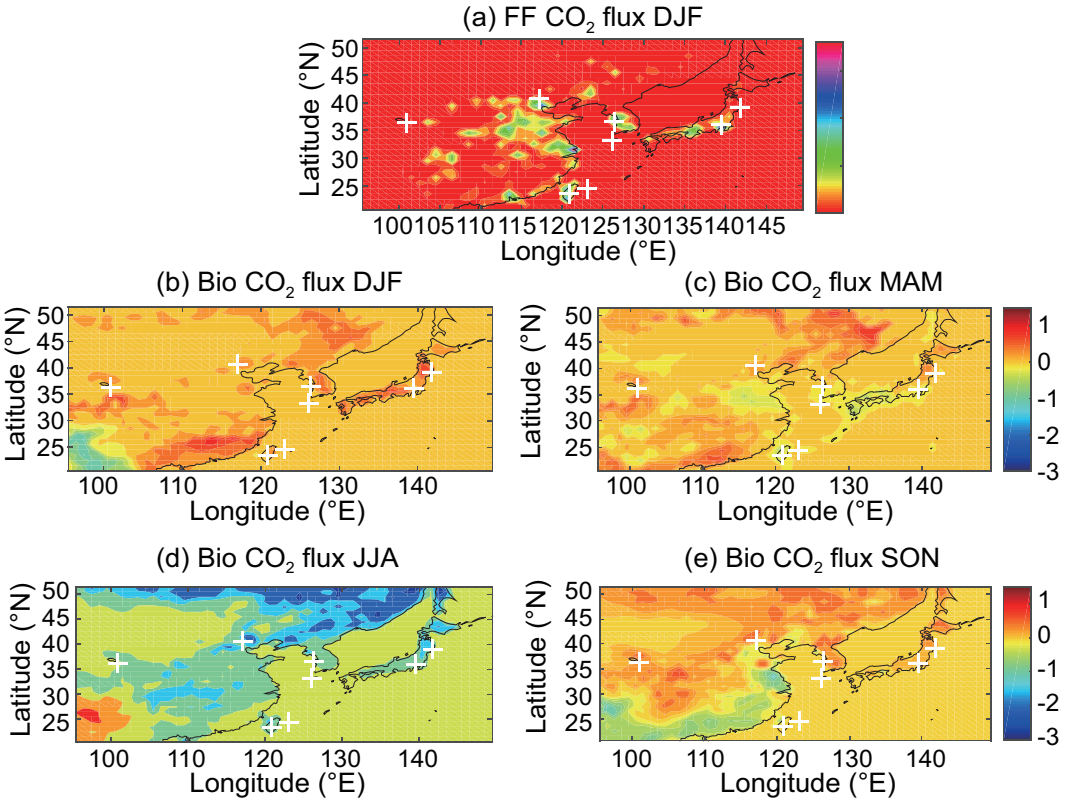

Fig. 3. Model-simulated seasonal mean CO_2 flux (units: μmol m^{-2} s^{-1}) (fossil fuels flux in the top panel and biospheric flux in the bottom four panels) during the period 2009–13. DJF, MAM, JJA and SON denote the winter (December–February), spring (March–May), summer (June–August) and autumn (September–November) seasons, respectively.

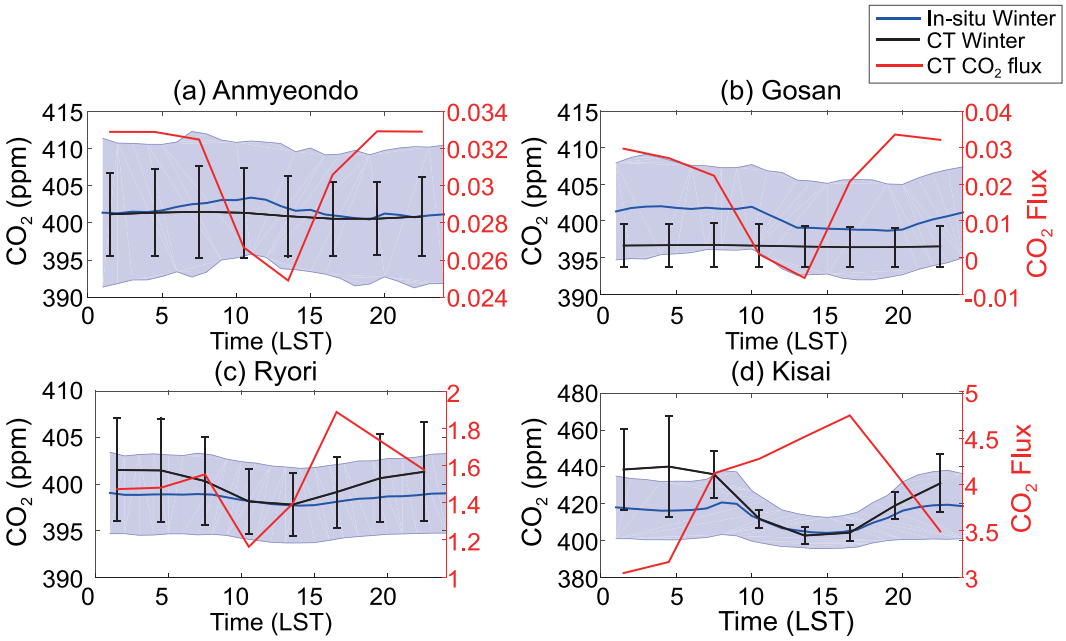

Fig. 4. Mean diurnal cycle of CO_2 in winter during 2009–13 (except for Gosan, which is in the period 2009–11). The blue curve shows the observed result and the black curve the model result. The $1-\sigma$ standard deviation is shown by the blue shading for the observations and by the black vertical lines for the model outputs. The red line represents the model-simulated CO_2 flux. Note: the scale of the y-axis is different.

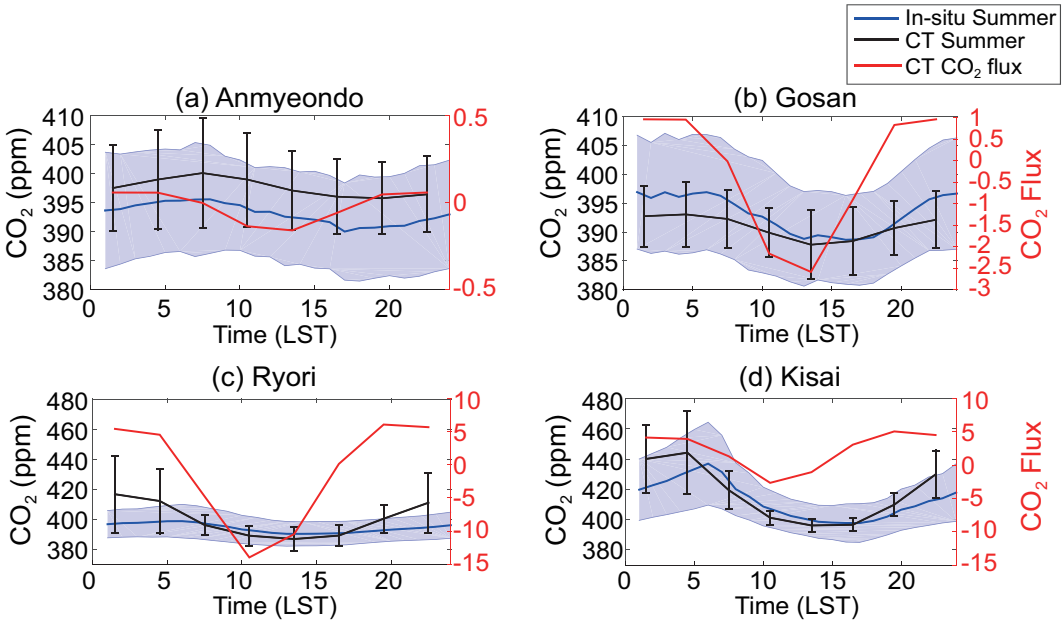

Fig. 5. As in Fig. 4 but for the summer season.

Table 2. Mean diurnal CO_2 concentrations (units: ppm) of the CT-Asia model, in-situ observations, and bias during winter and summer in the study period.

Station	Season	Model (mean ± std)	Observation (mean ± std)	Bias (model minus observation)
Anmyeondo	Winter	400.1 ± 0.2	399.9 ± 0.9	0.2
	Summer	396.7 ± 0.8	393.1 ± 1.9	3.6
Gosan	Winter	396.4 ± 0.2	399.5 ± 1.6	−3.1
	Summer	390.6 ± 1.3	393.2 ± 3.6	−2.6
Ryori	Winter	399.6 ± 1.4	398.4 ± 0.4	1.2
	Summer	398.5 ± 9.0	394.0 ± 2.6	4.5
Kisai	Winter	416.1 ± 9.6	409.8 ± 4.6	6.3
	Summer	415.2 ± 17.6	410.2 ± 11.2	5.0

Note: std, standard deviation.

Table 3. Daytime (1330–1630 LST) mean CO_2 concentrations (units: ppm) of the CT-Asia model, in-situ observations, and bias during winter and summer in the study period.

Station	Season	Model	Observation	Bias (model minus observation)
Anmyeondo	Winter	400.7	401.5	−0.8
	Summer	396.6	392.0	4.6
Gosan	Winter	396.5	398.9	−2.5
	Summer	388.1	389.1	−1.0
Ryori	Winter	398.5	397.8	0.7
	Summer	388.0	390.4	−2.4
Kisai	Winter	404.3	403.4	0.9
	Summer	396.6	398.1	−1.5

the prevailing wind directions were southwest and northwest, which brought airmasses rich with CO_2 from the land (see right-hand panels of Fig. S1 in the ESM). Furthermore, the standard deviation of the in-situ observations was higher than the model results, which reflects the influence of local emissions and sinks, typically playing a more important role in observed CO_2 concentrations at low wind speeds (Figs. S1, S2, and S3 in the ESM). Moreover, there was a strong terrestrial biospheric flux gradient around the station, where the signal was high compared to the corresponding nearest grid point. The bias was estimated to be 3.6 ppm in this particular season, as shown in Table 2.

Regarding Gosan station, located at the tip of the west coast of Jeju Island, it is too small to be captured by the resolution of the regional inverse model. This could also be a factor contributing to the differences between the simulation and observation. In summer, the in-situ observations depicted a large amplitude (peak-to-peak CO_2 concentrations) on the order of 8.3 ppm, while the model only produced an amplitude of 3.3 ppm, which was less than half that of the in-situ observations (see Fig. 5b).

Looking at Ryori and Kisai, the model exhibited a pronounced diurnal cycle in both winter and summer. The model exhibited good agreement in the afternoon at both stations, but a large discrepancy occurred at nighttime. This indicates that the model failed to simulate nocturnal CO_2 accumulations in both seasons. We can see almost comparable magnitudes of total simulated CO_2 flux (Figs. 5c and d) between 0000 and 0500 LST during summer at these stations. However, Kisai had a relatively elevated CO_2 concentration compared to Ryori. This might have been caused by underestimation of the nighttime boundary layer height and/or advection of CO_2 containing airmasses within this layer (Figs.S4 and S5 in the ESM). Some studies have examined the impact of planetary boundary layer height uncertainties on the modeled near-surface CO_2 concentrations during daytime, and estimated a bias of ~3 ppm (e.g., Kretschmer et al., 2012, 2014), while uncertainties in the horizontal winds can induce a to-

tal CO_2 transport uncertainty of ~6 ppm (Lin and Gerbig, 2005). At night, the representation error due to unresolved topography will be amplified within the nocturnal boundary layer (Tolk et al., 2008).

4.3. *Seasonal variations of CO_2*

Here, the ability of the model to reproduce the seasonal variations of CO_2 is evaluated through comparison with the in-situ observations at selected stations. The seasonal cycle amplitude, phase and bias were investigated. Examining the time offset of the seasonal cycle has important implications for flux estimates (Keppel-Aleks et al., 2012).

Figure 6 compares the seasonal cycle of the simulated CO_2 with the in-situ observations at selected stations. Daytime, nighttime, and all-hourly averaged data were considered separately. The in-situ data from Ryori, Yonagunijima, and Minamitorishima were assimilated in the CT2016 version, while the rest of the sites were independent of the CT2016 data assimilation system. Overall, the results for the seasonal cycle of the simulated CO_2 concentrations broadly agreed with the observations, with concentrations peaking in April and a minimum occurring in August/September. This result was found for all stations, when considering the daytime data. However, large discrepancies were identified when applying the nighttime data, in particular at Ryori, Kisai, and Shangdianzi. At Kisai and Shangdianzi, we quantified how well the model reproduced the seasonal variations when all daytime and nighttime data were incorporated; the correlation coefficients were 0.55 and 0.26 (Table 4 and Fig. 7), respectively. However, the result improved when considering only the daytime data, with correlation coefficients of about 0.84 and 0.71, and the biases were estimated to be -1.6 ± 3.2 and 5.3 ± 5.7 $(1-\sigma)$ ppm (see Table 5 and Fig. 6). This suggests that the inclusion of nighttime and early morning data affected the seasonal comparison.

Despite the overall agreement between the simulation and observations at Anmyeondo, it is evident that the model slightly overestimated the CO_2 concentrations during summertime. As noted in section 4.2, the diurnal variations of the simulated CO_2 concentrations at Anmyeondo during summer were estimated to be higher than the in-situ measurements. A mean bias of 1.2 ppm was found, with a corresponding standard deviation of 4.0 $(1-\sigma)$ ppm. The mismatch in the CO_2 seasonal amplitude indicates that the simulated CO_2 surface fluxes cannot capture the peak of the terrestrial carbon exchange (Yang et al., 2007).

Over the mountain stations, the seasonal cycles (Figs. 6g and h) indicated that the model overestimated the observations, with a pronounced phase difference. When applying the comparison method, the first vertical level in the model

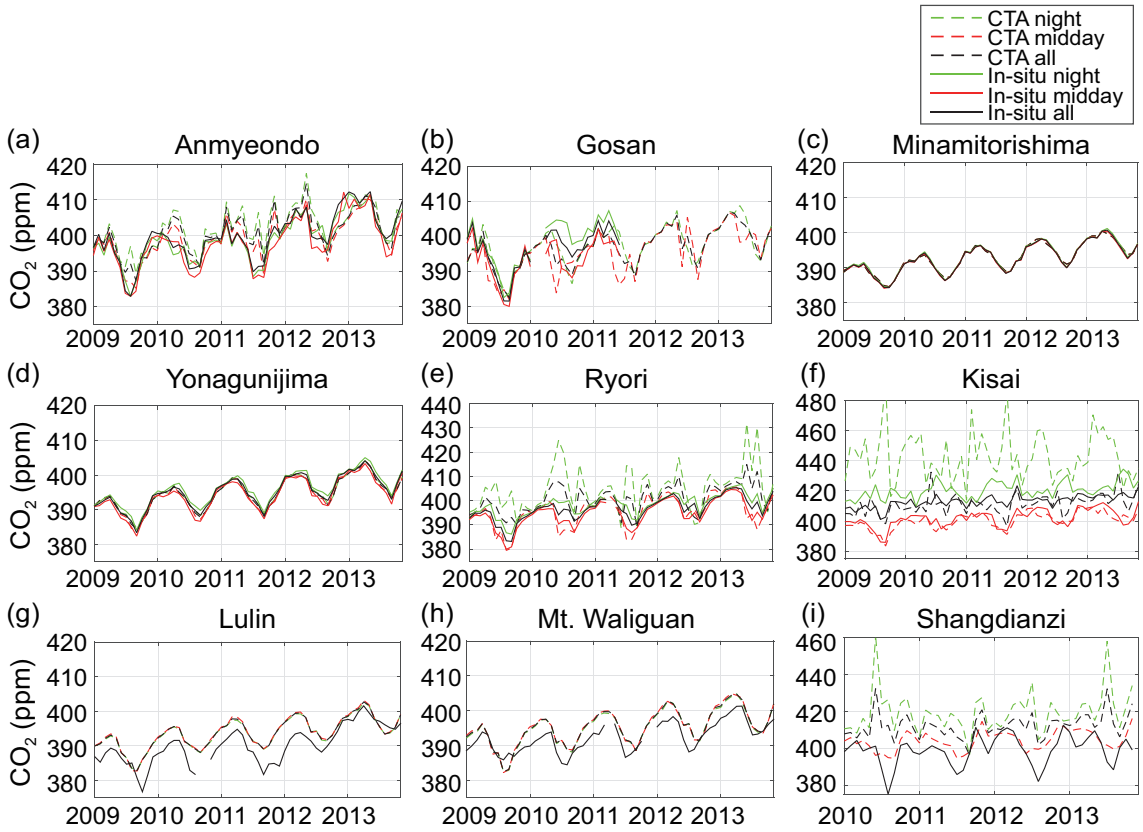

Fig. 6. Monthly time series of mean CO_2 concentrations for daytime, nighttime, and both day- and nighttime, during 2009–13 (except for Gosan, which is during 2009–11, and Shangdianzi, which is during 2010–13), as observed over selected sites in East Asia. Note that the in-situ monthly mean time series are not depicted specifically for daytime and nighttime at Lulin, Mt. Waliguan, and Shangdianzi.

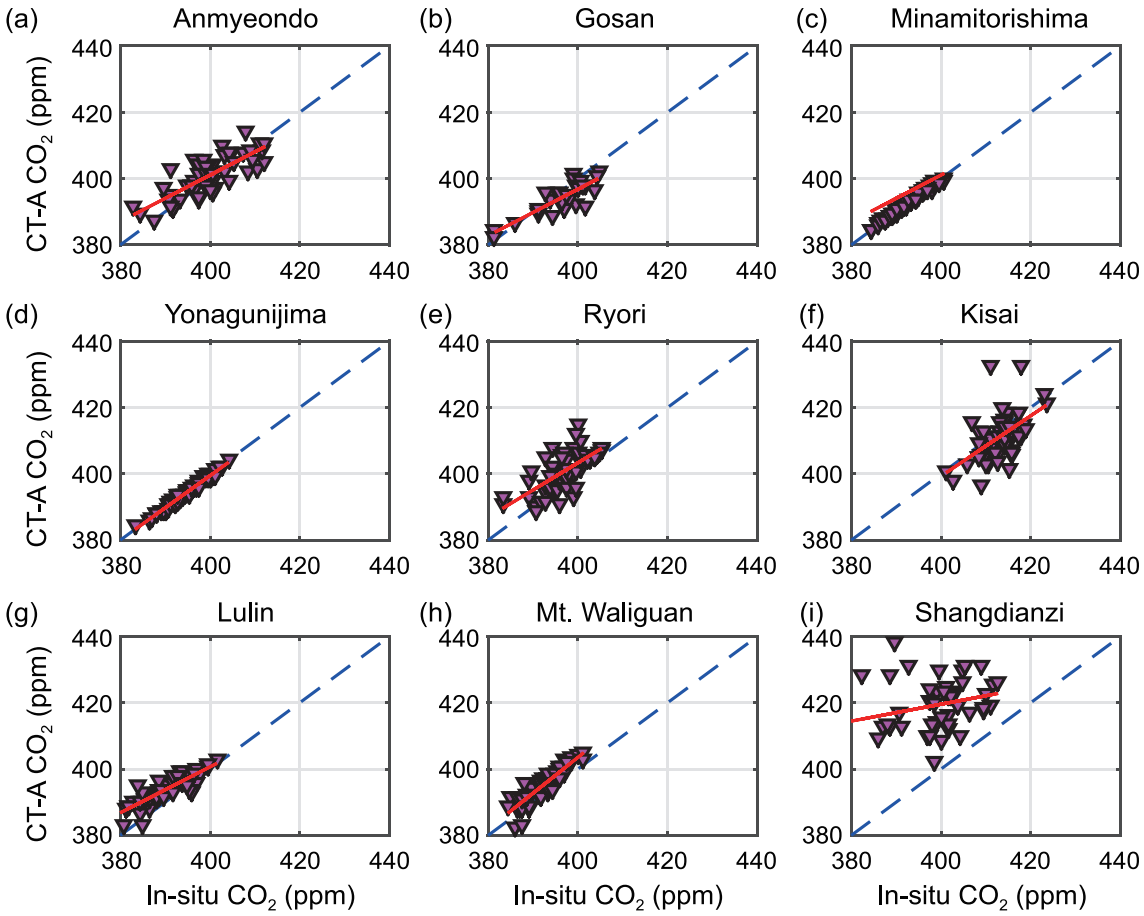

Fig. 7. Model-simulated versus in-situ observed monthly mean (includes all hourly values) CO_2 concentrations during 2009–13 (except for Gosan, which is during 2009–11, and Shangdianzi, which is during 2010–13), as observed at nine selected sites in East Asia. The blue dashed line is the 1:1 fitting line. See Table 4 for the statistical results.

did not match with the in-situ inlet height, because the model resolution could not resolve the topography of such complex terrain accurately (see Fig. 1). Consequently, we selected the model vertical level that approximately represented the in-situ inlet height above sea level (i.e. the fifth vertical level for Mt. Waliguan and the eighth for Lulin). The slight mismatch in the model sampling vertical level with the in-situ inlet height may have had an impact on the phase difference and bias in the seasonal cycle, probably because of the timing difference in the transport process. For example, at Mt. Waliguan, the peak often occurred earlier than observed, whereas the minimum occurred later. Fang et al. (2014) noticed the occurrence of seasonal CO_2 maximum periods fluctuate considerably, ranging from December at Longfengshan and Lin'an, to March for Shangdianzi and May for Mt. Waliguan. This difference is believed to be driven not only

Table 4. Statistical comparison of atmospheric CO_2 concentrations (units: ppm) between the in-situ observations and CT-Asia model on a monthly mean basis (includes all hourly values) during the study period.

Station	N	R	R^2	Bias ± std	RMSE	Slope	Intercept
Anmyeondo	59	0.79	0.62	1.2 ± 4.0	4.2	0.70	120.5
Gosan	28	0.85	0.72	−2.1 ± 3.2	3.8	0.70	116.2
Ryori	58	0.66	0.43	3.9 ± 4.5	5.9	0.82	75.3
Kisai	59	0.55	0.30	−1.9 ± 5.8	6.0	0.91	34.6
Minamitorishima	59	0.99	0.98	0.1 ± 0.5	0.5	0.97	13.2
Yonagunjima	59	0.99	0.99	−0.4 ± 0.7	0.8	0.97	11.2
Lulin	57	0.87	0.76	3.7 ± 2.7	4.6	0.69	123.8
Mt. Waliguan	56	0.89	0.79	3.9 ± 2.3	3.7	1.08	−28.3
Shangdianzi	47	0.26	0.07	20.1 ± 9.7	22.3	0.25	317.6

Note: std, standard deviation.

Table 5. As in Table 4 but for daytime (1330–1630 LST).

Station	N	R	R^2	Bias ± std	RMSE	Slope	Intercept
Anmyeondo	59	0.88	0.77	1.3 ± 3.3	3.5	0.76	96.3
Gosan	28	0.70	0.49	−0.3 ± 4.5	4.4	0.66	135.5
Ryori	58	0.93	0.86	0.7 ± 2.5	2.6	1.12	−46.7
Kisai	59	0.84	0.71	−1.6 ± 3.2	3.6	0.79	82.5
Minamitorishima	59	0.99	0.98	0.2 ± 0.5	0.5	0.97	11.7
Yonagunjima	59	0.99	0.98	−0.3 ± 0.8	0.9	0.96	15.6
Shangdianzi	47	0.71	0.50	5.3 ± 5.7	7.7	0.47	218.7

Note: std, standard deviation.

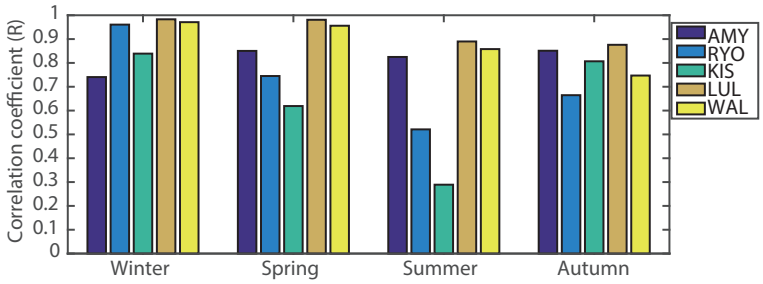

Fig. 8. Correlation coefficient (model versus in-situ observations) for the CO_2 concentration in each season at Anmyeondo, Ryori, Kisai, Lulin, and Mt. Waliguan during 2009–13.

by regionally different terrestrial ecosystems and human activities, but also by local meteorological conditions (Zhang et al., 2008). At Mt. Waliguan and Lulin, we found a good level of agreement in capturing the variability of the observations, with correlation coefficients of 0.89 and 0.87, respectively. Both stations exhibited positive biases, with estimated values of 3.7 (Mt. Waliguan) and 3.9 ppm (Lulin). At remote stations like Minamitorishima and Yonagunijima, a very good level agreement was obtained, with a correlation coefficient of 0.99 and an RMSE less than 0.79.

We also determined the correlation coefficients for Anmyeondo, Ryori, Kisai, Lulin, and Mt. Waliguan, for each season (Fig. 8). Kisai revealed a poor correlation ($R = 0.29$) in summer, whereas a good correlation was found in winter (0.84). Ryori showed similar results, with a correlation of 0.52 in summer and 0.96 in winter. This suggests that the model's performance in capturing the monthly variations for each season varies, with better representation of winter than other seasons. The model's ability in capturing the effect of terrestrial vegetation, particularly in the peak growing season, needs further improvement.

5. Conclusions

The performance of a nested-grid CT model in simulating atmospheric CO_2 concentrations was assessed through comparison with in-situ observations over nine selected stations in East Asia during the period 2009–13. The evaluation was conducted in terms of diurnal and seasonal variations, in which the amplitude, phase differences and bias were examined. The diurnal cycles of terrestrial biospheric fluxes and the planetary boundary layer were the most likely deriving factors for the variations of surface level CO_2 concentrations.

Large discrepancies existed with regard to the diurnal cycle at night when comparing the observations and model results in winter and summer, as inferred from data at four stations (Anmyeondo, Gosan, Ryori, and Kisai). In general, the model's ability to reproduce the CO_2 diurnal cycle remains challenging. On the other hand, the model exhibited a very good level of agreement with observations in daytime at those target stations. Overall, biases were less than 6.3 ppm on an all-hourly mean basis, and this was further reduced to a maximum of 4.6 ppm when considering only daytime. For example, at Anmyeondo, a small bias was obtained in winter, on the order of 0.2 ppm, whereas in summertime the bias was higher. The observed large discrepancy at nighttime might be reduced by increasing the horizontal resolution and vertical levels.

In terms of seasonal variation, the level of agreement was judged by considering daytime, nighttime, and all-hourly averaged data. The overall performance of the model in reproducing the observed seasonal variations of CO_2 all-hourly averaged basis was good at most sites, with the exception of Ryori, Kisai, and Shangdianzi stations. The level of agreement was further improved at almost all stations when considering the comparison during daytime, with a correlation coefficient ranging from 0.70 to 0.99; however, the model performed poorly in capturing the peak drawdown of CO_2 during the summer season at Shangdianzi. Choosing the model sampling level that corresponded to the in-situ inlet height may have led to a small overestimation or underestimation of CO_2; however, this particular effect was observed mainly over mountainous areas.

The findings of this study highlight the strengths and weaknesses of the model in reproducing diurnal and seasonal variations of near-surface CO_2 concentrations. We recommend that continued efforts are made to evaluate the model's performance, particularly in capturing nighttime observations. Also, a series of model experiments are required in the future in order to explicitly quantify the biases in the simulated near-surface CO_2 concentrations on the diurnal time scale in relation to meteorological parameters (e.g., boundary layer height, wind speed and direction, relative humidity).

Acknowledgements. This work was supported by the Korea Meteorological Administration Research and Development Program "Research and Development for KMA Weather, and Earth system Services-Development and Assessment of AR6 Climate Change Scenarios" under Grant (KMA2018-00321). We gratefully acknowledge those who provided the access to the in-situ data at the WDCGG (https://ds.data.jma.go.jp/gmd/wdcgg/cgi-bin/wdcgg/catalogue.cgi).

Electronic supplementary material. Supplementary material

is available in the online version of this article at https://doi.org/10.1007/s00376-019-8150-x.

REFERENCES

Ahmadov, R., C. Gerbig, R. Kretschmer, S. Körner, C. Rödenbeck, P. Bousquet, and M. Ramonet, 2009: Comparing high resolution WRF-VPRM simulations and two global CO_2 transport models with coastal tower measurements of CO_2. *Biogeosciences*, **6**, 807–817, https://doi.org/10.5194/bg-6-807-2009.

Andrews, A. E., and Coauthors, 2014: CO_2, CO, and CH_4 measurements from tall towers in the NOAA Earth System Research Laboratory's Global Greenhouse Gas Reference Network: Instrumentation, uncertainty analysis, and recommendations for future high-accuracy greenhouse gas monitoring efforts. *Atmospheric Measurement Techniques*, **7**, 647–687, https://doi.org/10.5194/amt-7-647-2014.

Baker, D. F., and Coauthors, 2006: TransCom 3 inversion intercomparison: Impact of transport model errors on the interannual variability of regional CO_2 fluxes, 1988–2003. *Global Biogeochemical Cycles*, **20**, GB1002, https://doi.org/10.1029/2004GB002439.

Bakwin, P. S., P. P. Tans, D. F. Hurst, and C. L. Zhao, 1998: Measurements of carbon dioxide on very tall towers: Results of the NOAA/CMDL program. *Tellus*, **50B**, 401–415, https://doi.org/10.3402/tellusb.v50i5.16216.

Ballav, S., and Coauthors, 2012: Simulation of CO_2 concentration over East Asia using the regional transport model WRF-CO_2. *J. Meteor. Soc. Japan*, **90**(6), 959–976, https://doi.org/10.2151/jmsj.2012-607.

Cheng, S. Y., L. X. Zhou, P. P. Tans, X. Q. An, and Y. S. Liu, 2018: Comparison of atmospheric CO_2 mole fractions and source–sink characteristics at four WMO/GAW stations in China. *Atmos. Environ.*, **180**, 216–225, https://doi.org/10.1016/j.atmosenv.2018.03.010.

Cheng, Y. L., X. Q. An, F. H. Yun, S. X. Fang, L. Xu, L. X. Zhou, and L. X. Liu, 2013: Simulation of CO_2 variations at Chinese background atmospheric monitoring stations between 2000 and 2009: Applying a CarbonTracker model. *Chinese Science Bulletin*, 2013, **58**, 3986–3993, https://doi.org/10.1007/s11434-013-5895-y.

Dee, D. P., and Coauthors, 2011: The ERA-Interim reanalysis: Configuration and performance of the data assimilation system. *Quart. J. Roy. Meteor. Soc.*, **137**, 553–597, https://doi.org/10.1002/qj.828.

Fang, S. X., L. X. Zhou, P. P. Tans, P. Ciais, M. Steinbacher, L. Xu, and T. Luan, 2014: In situ measurement of atmospheric CO_2 at the four WMO/GAW stations in China. *Atmospheric Chemistry and Physics*, **14**, 2541–2554, https://doi.org/10.5194/acp-14-2541-2014.

Fukuyama, Y., 2013: Atmospheric CO_2 monthly concentration data, Yonagunijima, World Data Centre for Greenhouse Gases. Japan Meteorology Agency, Tokyo. [Available online at http://ds.data.jma.go.jp/gmd/wdcgg/.]

Gerbig, C., S. Körner, and J. C. Lin, 2008: Vertical mixing in atmospheric tracer transport models: Error characterization and propagation. *Atmospheric Chemistry and Physics*, **8**, 591–602, https://doi.org/10.5194/acp-8-591-2008.

Gurney, K. R., and Coauthors, 2002: Towards robust regional estimates of CO_2 sources and sinks using atmospheric transport models. *Nature*, **415**, 6872, 626–630, https://doi.org/10.1038/415626a.

Hansen, J., and Coauthors, 2007: Dangerous human-made interference with climate: A GISS modelE study. *Atmospheric Chemistry and Physics*, **7**, 2287–2312, https://doi.org/10.5194/acp-7-2287-2007.

IPCC, 2013: *Climate Change 2013*: *The Physical Science Basis*, *Contribution of Working Group I to the Fifth Assessment Report of the Intergovernmental Report on Climate Change*. Cambridge University Press, United Kingdom and New York, NY, USA, 1535 pp.

Keeling, C. D., R. B. Bacastow, A. F. Carter, S. C. Piper, T. P. Whorf, M. Heimann, M. W. G. Mook, and H. Roeloffzen, 1989: *A Three Dimensional Model of Atmospheric CO_2 Transport Based on Observed Winds*. *I*: *Analysis of Observed Data*. American Geophysical Union, Washington D. C., 165–236.

Keppel-Aleks, G., and Coauthors, 2012: The imprint of surface fluxes and transport on variations in total column carbon dioxide. *Biogeosciences*, **9**, 875–891, https://doi.org/10.5194/bg-9-875-2012.

Kretschmer, R., C. Gerbig, U. Karstens, and F.-T. Koch, 2012: Error characterization of CO_2 vertical mixing in the atmospheric transport model WRF-VPRM. *Atmospheric Chemistry and Physics*, **12**, 2441–2458, https://doi.org/10.5194/acp-12-2441-2012.

Kretschmer, R., C. Gerbig, U. Karstens, G. Biavati, A. Vermeulen, F. Vogel, S. Hammer, and K. U. Totsche, 2014: Impact of optimized mixing heights on simulated regional atmospheric transport of CO_2. *Atmospheric Chemistry and Physics*, **14**, 7149–7172, https://doi.org/10.5194/acp-14-7149-2014.

Krol, M., S., and Coauthors, 2005: The two-way nested global chemistry-transport zoom model TM5: Algorithm and applications. *Atmospheric Chemistry and Physics*, **5**, 417–432, https://doi.org/10.5194/acp-5-417-2005.

Law, R. M., and Coauthors, 2008: TransCom model simulations of hourly atmospheric CO_2: Experimental overview and diurnal cycle results for 2002. *Global Biogeochemical Cycles*, **22**, GB3009, https://doi.org/10.1029/2007GB003050.

Lin, J. C., and C. Gerbig, 2005: Accounting for the effect of transport errors on tracer inversions. *Geophys. Res. Lett.*, **32**, L01802, https://doi.org/10.1029/2004GL021127.

Patra, P. K., and Coauthors, 2008: TransCom model simulations of hourly atmospheric CO_2: Analysis of synoptic-scale variations for the period 2002–2003. *Global Biogeochemical Cycles*, **22**, GB4013, https://doi.org/10.1029/2007GB003081.

Peters, W., and Coauthors, 2007: An atmospheric perspective on North American carbon dioxide exchange: CarbonTracker. *Proceedings of the National Academy of Sciences of the United States of America*, **104**, 18 925–18 930, https://doi.org/10.1073/pnas.0708986104.

Peters, W., and Coauthors, 2010: Seven years of recent European net terrestrial carbon dioxide exchange constrained by atmospheric observations. *Global Change Biology*, **16**, 1317–1337, https://doi.org/10.1111/j.1365-2486.2009.02078.x.

Prather, M. J., X. Zhu, S. E. Strahan, S. D. Steenrod, and J. M. Rodriguez, 2008: Quantifying errors in trace species transport modeling. *Proceedings of the National Academy of Sciences of the United States of America*, **105**, 19 617–19 621, https://doi.org/10.1073/pnas.0806541106.

Qu, Y., and Coauthors, 2013: Comparison of atmospheric CO_2 observed by GOSAT and two ground stations in China. *Int. J. Remote Sens.*, **34**(11), 3938–3946, https://doi.org/10.1080/

01431161.2013.768362.

Sasaki, H., 2006: Atmospheric CO_2 hourly concentration data. Minamitorishima, Ryori and Yonagunijima, World Data Centre for Greenhouse Gases, Japan Meteorological Meteorological Agency. [Available online from http://gqw.kishou.go.jp/wdcgg.html]

Shim, C., J. Lee, and Y. X. Wang, 2013: Effect of continental sources and sinks on the seasonal and latitudinal gradient of atmospheric carbon dioxide over East Asia. *Atmos. Environ.*, **79**, 853–860, https://doi.org/10.1016/j.atmosenv.2013.07.055.

Swathi, P. S., N. K. Indira, P. J. Rayner, M. Ramonet, D. Jagadheesha, B. C. Bhatt, and V. K. Gaur, 2013: Robust inversion of carbon dioxide fluxes over temperate Eurasia in 2006–2008. *Current Science*, **105**, 201–208.

Takahashi, T., and Coauthors, 2009: Climatological mean and decadal change in surface ocean pCO2, and net sea-air CO_2 flux over the global oceans. *Deep Sea Research Part II*: *Topical Studies in Oceanography*, **56**(8–10), 554–577, http://dx.doi.org/10.1016/j.dsr2.2008.12.009.

Tans, P. P., I. Y. Fung, and T. Takahashi, 1990: Observational constraints on the global atmospheric CO_2 budget. *Science*, **247**(4949), 1431–1438, https://doi.org/10.1126/science.247.4949.1431.

Tian, H. Q., and Coauthors, 2016: The terrestrial biosphere as a net source of greenhouse gases to the atmosphere. *Nature*, **531**, 225–228, https://doi.org/10.1038/nature16946.

Tolk, L. F., A. G. C. A. Meesters, A. J. Dolman, and W. Peters, 2008: Modelling representation errors of atmospheric CO_2 mixing ratios at a regional scale. *Atmospheric Chemistry and Physics*, **8**, 6587–6596, https://doi.org/10.5194/acp-8-6587-2008.

Watson, A. J., N. Metzl, and U. Schuster, 2011: Monitoring and interpreting the ocean uptake of atmospheric CO_2. *Philosophical Transactions of the Royal Society A*, **369**, 1997–2008, https://doi.org/10.1098/rsta.2011.0060.

Yang, Z., R. A. Washenfelder, G. Keppel-Aleks, N. Krakauer, J. T. Randerson, P. P. Tans, C. Sweeney, and P. O. Wennberg, 2007: New constraints on Northern Hemisphere growing season net flux. *Geophys. Res. Lett.*, **34**, L12807, https://doi.org/10.1029/2007GL029742.

Zhang, D. Q., and Coauthors, 2008: Temporal and spatial variations of the atmospheric CO_2 concentration in China. *Geophys. Res. Lett.*, **35**, L03801, https://doi.org/10.1029/2007GL032531.

Zhou, L. X., D. E. J. Worthy, P. M. Lang, M. K. Ernst, X. C. Zhang, Y. P. Wen, and J. L., 2004: Ten years of atmospheric methane observations at a high elevation site in Western China. *Atmos. Environ.*, **38**, 7041–7054, https://doi.org/10.1016/j.atmosenv.2004.02.072.

Zhou, L. X., J. W. C. White, T. J. Conway, H. Mukai, K. MacClune, X. C. Zhang, Y. P. Wen, and J. L. Li, 2006: Long-term record of atmospheric CO_2 and stable isotopic ratios at Waliguan Observatory: Seasonally averaged 1991–2002 source/sink signals, and a comparison of 1998–2002 record to the 11 selected sites in the Northern Hemisphere. *Global Biogeochemical Cycles*, **20**, GB2001, https://doi.org/10.1029/2004GB002431.